Ectomycorrhizal fungal decay traits along a soil nitrogen gradient

Peter T. Pellitier[1] **and Donald R. Zak**[1,2]

[1]School for Environment and Sustainability, University of Michigan, Ann Arbor, MI 48109, USA; [2]Department of Ecology and Evolutionary Biology, University of Michigan, Ann Arbor, MI 48109, USA

Author for correspondence:
Peter T. Pellitier
Email: ptpell@stanford.edu

Received: *18 May 2021*
Accepted: *16 August 2021*

New Phytologist (2021) **232:** 2152–2164
doi: 10.1111/nph.17734

Key words: community aggregated traits, community assembly, ectomycorrhizal fungi, organic nitrogen, shotgun metagenomics, soil gradient, soil organic matter (SOM).

Summary

- The extent to which ectomycorrhizal (ECM) fungi decay soil organic matter (SOM) has implications for accurately predicting forest ecosystem response to climate change. Investigating the distribution of gene traits associated with SOM decay among ectomycorrhizal fungal communities could improve understanding of SOM dynamics and plant nutrition. We hypothesized that soil inorganic nitrogen (N) availability structures the distribution of ECM fungal genes associated with SOM decay and, specifically, that ECM fungal communities occurring in inorganic N-poor soils have greater SOM decay potential.
- To test this hypothesis, we paired amplicon and shotgun metagenomic sequencing of 60 ECM fungal communities associating with *Quercus rubra* along a natural soil inorganic N gradient.
- Ectomycorrhizal fungal communities occurring in low inorganic N soils were enriched in gene families involved in the decay of lignin, cellulose, and chitin. Ectomycorrhizal fungal community composition was the strongest driver of shifts in metagenomic estimates of fungal decay potential. Our study simultaneously illuminates the identity of key ECM fungal taxa and gene families potentially involved in the decay of SOM, and we link rhizomorphic and medium-distance hyphal morphologies with enhanced SOM decay potential.
- Coupled shifts in ECM fungal community composition and community-level decay gene frequencies are consistent with outcomes of trait-mediated community assembly processes.

Introduction

Accurate understanding of microbial community assembly and function (Nemergut *et al.*, 2013) is critical to their incorporation into predictive biogeochemical models (Hall *et al.*, 2018; Fry *et al.*, 2019; Bradford *et al.*, 2021). Trait-based frameworks developed for plant ecology (Diaz *et al.*, 1998; Cornwell & Ackerly, 2009) can be applied to investigate microbial community assembly (Fierer *et al.*, 2014; Malik *et al.*, 2020a). For example, plant traits subject to environmental filtering have been inferred by analyzing community-level trait distributions along abiotic gradients (Cornwell & Ackerly, 2009; Bernard-Verdier *et al.*, 2012). Such patterns are predicted to occur because functional trait trade-offs can constrain the viable life-history strategies present in individual taxa. Environmental filters may act on this variation, leading to convergent or 'underdispersed' local trait distributions and significant associations between environmental conditions and species functional traits (Diaz *et al.*, 1998; Ackerly & Cornwell, 2007). While trait trade-offs are increasingly characterized for a wide range of microbial taxa (Malik *et al.*, 2020a,b; Zanne *et al.*, 2020), there remains minimal understanding of the role of functional traits in microbial community assembly processes (Bouma-Gregson *et al.*, 2019; Maynard *et al.*, 2019; Rath *et al.*, 2019).

Microbial communities, especially root mutualists, serve to modify root physiology and plant fitness across environmental conditions (Peay, 2016; Fitzpatrick *et al.*, 2018; Ravanbakhsh *et al.*, 2019). Ectomycorrhizal (ECM) fungi, in particular, dominate boreal and temperate forest soil microbial communities, providing plant hosts with the majority of their annual nitrogen (N) requirements (*c.* 70%) (Smith & Read, 2010). Despite being one of the most studied microbial groups, understanding of the distribution of ECM fungal traits remain poorly understood (Courty *et al.*, 2016; van der Linde *et al.*, 2018; Meeds *et al.*, 2021). One prominent ECM fungal functional trait is the acquisition of N bound in soil organic matter (N-SOM), which constitutes the majority of soil N (Vitousek & Howarth, 1991). ECM fungal access to and assimilation of N-SOM is contingent upon the decay of plant and microbially derived compounds present in SOM (Lindahl & Tunlid, 2015; Zak *et al.*, 2019b; Lehmann *et al.*, 2020). Historically only inorganic N and certain simple organic N sources were considered accessible to plants (Schimel & Bennett, 2004); however, recent studies suggest that certain ECM fungi allow plants to acquire N-SOM, thereby 'short-circuiting' inorganic N cycling (Lindahl & Tunlid, 2015; Zak *et al.*, 2019b). ECM fungal decay capacity has profound implications for ecosystem function. For example, plant acquisition of N-SOM is one of the most sensitive parameters determining global forest productivity responses to elevated CO_2 (Terrer *et al.*, 2016, 2021), and may also impact SOM dynamics at global scales (Orwin *et al.*, 2011; Averill *et al.*, 2014; Sulman *et al.*,

2019). Despite these emergent findings, factors controlling SOM decay capacity among ECM fungal communities remains poorly understood.

Studies at local, regional, and continental scales consistently identify soil inorganic N availability as a key determinant of ECM fungal community composition (Taylor *et al.*, 2000; Lilleskov *et al.*, 2002a; Peay *et al.*, 2015; van der Linde *et al.*, 2018). Biological market perspectives provide insight into how N availability and fungal N acquisition traits may interact to structure these communities (Koide *et al.*, 2014; Christian & Bever, 2018). Plants may partner with fungal mutualists that maximize N (or phosphorus) acquisition, while minimizing photosynthate expenditure (Hortal *et al.*, 2017; Bogar *et al.*, 2019; Meeds *et al.*, 2021). Comparative genomic analyses suggest that ECM fungal decay potential varies widely across the *c.* 80 independent evolutionary originations of the ECM fungal lifestyle (Kohler *et al.*, 2015; Shah *et al.*, 2016; Pellitier & Zak, 2018). Accordingly, if the metabolic cost of SOM decay and N-SOM acquisition is high relative to inorganic N acquisition (Hammel & Cullen, 2008; Janusz *et al.*, 2017), ECM fungi with greater SOM decay capacity may be disfavored under certain environmental contexts (Koide *et al.*, 2014). In this study we investigate the outcome of trait-mediated assembly processes that structure the distribution of ECM fungal SOM decay traits and ECM fungal communities along a natural soil inorganic N gradient. We specifically predict that ECM fungal communities occurring in low inorganic N soils are compositionally distinct and have greater genomic potential to decay SOM and access the N therein.

Gene-based calculation of community aggregated traits – which are conceptually similar to widely used measures of community weighted mean trait values for plant communities (Cornwell & Ackerly, 2009; Bernard-Verdier *et al.*, 2012) – can also be used to assess community-level microbial properties (Fierer *et al.*, 2014). Because ECM fungi use decay mechanisms retained from their saprotrophic ancestors (Lindahl & Tunlid, 2015; Pellitier & Zak, 2018), genes found in saprotrophic fungal genomes encoding hydrolytic and oxidative enzymes, as well as Fenton-based decay mechanisms, are likely involved in ECM fungal degradation of SOM (Doré *et al.*, 2015; Kohler *et al.*, 2015; Nicolás *et al.*, 2019; Floudas *et al.*, 2020). In most cases, however, the identity and activity of specific gene families, particularly under field conditions, remain unknown (Zak *et al.*, 2019b). It may be possible to derive the identity of key gene families, if those associated with SOM decay impact fungal persistence within a community (i.e. are functional) (Violle *et al.*, 2007). Accordingly, shifts in the relative abundance of certain gene families along the soil inorganic N gradient could represent the outcome of assembly processes that favored or disfavored their suitability.

We studied ECM fungal communities inhabiting 60 even-aged *Quercus rubra* trees arrayed along a natural inorganic N gradient in a temperate upland forest ecosystem. We used amplicon sequencing to characterize shifts in ECM fungal communities and and used shotgun metagenomic sequencing to calculate community aggregated decay trait (CADT) profiles. We identified linkages between 100 individual gene families and soil inorganic N availability using an extension of indicator species (gene) analysis (Baker & King, 2010). Our use of a single and even-aged host (*c.* 100 yr old) eliminates the potentially confounding effect of host specificity and ontogeny in fungal community assembly (van der Linde *et al.*, 2018; Wasyliw & Karst, 2020).

For fungal gene families that are primarily involved in SOM decay, we hypothesize negative correlations with increasing soil inorganic N availability. Certain gene families in particular are predicted to exhibit the strongest negative correlations with soil inorganic N availability. Specifically, extracellular class II peroxidases appear critical to ECM fungal decay under laboratory and field conditions (Bödeker *et al.*, 2014; Sterkenburg *et al.*, 2018; Lindahl *et al.*, 2021). Manganese peroxidases (MnPs), lignin peroxidase, and dye-decoloring peroxidases evolved exclusively in the Agaricomycetes and have some of the greatest known oxidative capacity to decay SOM (Janusz *et al.*, 2017). These genes are present at relatively high abundance in certain ECM fungal genomes, such as the widespread genus *Cortinarius* (Bödeker *et al.*, 2009; Miyauchi *et al.*, 2020). Additionally, genes encoding extracellular lytic polysaccharide monooxygenases (LPMOs) are upregulated in ECM fungal hyphae in the presence of SOM (Nicolás *et al.*, 2019). Finally, cellobiose dehydrogenases (CDHs) are almost exclusively produced by white-rot saprotrophic fungi; for ECM fungi that originated from such lineages, CDHs may play a substantial role in the decay of SOM (Doré *et al.*, 2015; Janusz *et al.*, 2017). By contrast, genes with primarily intracellular roles, such as those involved in the initiation of the mycorrhizal symbiosis or fungal cell wall remodeling, may not exhibit significant shifts along the soil inorganic N gradient.

Materials and Methods

Site descriptions

Sixty mature *Quercus rubra* L. individuals were sampled across a natural mosaic of soil inorganic N availabilities in Manistee National Forest in northwestern Lower Michigan (Supporting Information Fig. S1). The trees studied here are approximately even aged resulting from regrowth following forest clearing in the early 20th century; forests in this region have subsequently been free of anthropogenic disturbance. Five mature *Q. rubra* individuals that were at least 10 m apart were sampled within a total of 12 forest stands; previous studies indicate that these stands broadly span the range of soil nutrient availabilities in this region (Zak *et al.*, 1986; Zak & Pregitzer, 1990). Variation in nutrient cycling is derived from microsite climatic differences in nutrient and water retention that have developed in the past *c.* 10 000 yr, and all focal trees occur within an elevation band of 70–130 m (Zak *et al.*, 1986). Relative differences in soil nutrient availability among soils have persisted for decades (Zak *et al.*, 1986; Zak & Pregitzer, 1990). Soils across the study region are uniformly derived from sandy (*c.* 85% sand) glacial drift; and because the sampling region is relatively small, with the most distant sites being *c.* 50 km apart (Fig. S1), macroclimatic differences are minimal. Annual rates of net N mineralization (an estimate of

inorganic N availability) range from 38 to 120 kg ha^{-1} yr^{-1} – calculated from Zak & Pregitzer (1990) – which broadly spans soil inorganic N availability in the upper Lake States region (Pastor *et al.*, 1984; McClaugherty *et al.*, 1985). N deposition in the study region, based on National Atmospheric Deposition Program estimates (year 2016), is *c.* 3 kg ha^{-1}, primarily in the form of ammonium (NH_4^+). Foliar N concentrations of the focal trees increased with soil mineralization rates, ranging from 21 to 29 mg g^{-1} (Pellitier *et al.*, 2021a). The regional scale (*c.* 50 km) of this study may reduce the potential for dispersal limitation to be an overwhelming impact on community assembly (Peay *et al.*, 2012), such that observed patterns in species and trait distributions primarily represent the outcome of differential biotic and abiotic filters on community assembly (Ackerly, 2003). See Methods S1 for further information.

Soil characterization

In August 2018, ECM fungal root-tips were collected radially around the dripline of each focal *Q. rubra* individual; cores were 10 cm deep and 121 cm^2 (11 × 11 cm^2), and all five cores collected for each tree were kept intact until dissection. Soil cores for physicochemical analysis were collected immediately adjacent to the root-tip cores in both May and August 2018, but were 5 cm diameter and 10 cm deep. The O_i horizon was removed where present, ranging from 0.24 to 2 cm across stands. Soil net N mineralization rates, soil carbon (C) and N, pH, total free primary amines (TFPAs), and gravimetric soil water content were measured from these soil cores. In addition, all overstory plant stems > 5 cm diameter breast height (DBH), within 10 m of each focal *Q. rubra* stem, were identified and measured at DBH. A total of 1304 nonfocal tree stems were inventoried. See Methods S1 for further detail.

Isolating ectomycorrhizal fungal root-tips

Briefly, root-tip cores were pooled for each individual focal tree, and root-tips were manually excised using a dissecting microscope after visually eliminating non-*Quercus* roots. Sampling was standardized by visually assessing the tips of *c.* 90% (wet weight) of all *Quercus* roots in each of the root cores. In total, 14 944 ECM fungal root-tips were excised. DNA was extracted from lyophilized tissue using a Qiagen DNeasy Plant Mini Kit, and DNA pools were split for subsequent amplicon and metagenomic sequencing. See Methods S1 for further detail.

PCR and fungal taxonomy

The ITS2 fragment of ribosomal RNA was amplified using PCR, following Taylor *et al.* 2016, and sequenced using Illumina MiSeq (2 × 250 bp; San Diego, CA, USA). Sequences were processed using DADA2, and amplicon sequence variants (ASVs) were assigned taxonomy using the UNITE dynamic database (v.8; 97–99% sequence similarity) (Callahan *et al.*, 2016; Nilsson *et al.*, 2019). The mycorrhizal status of fungal genera was assigned using literature searches (Tedersoo & Smith, 2013), and genera with mixed, unidentified, or non-ECM fungal status were removed from subsequent analyses (*c.* 5% of overall sequences). We used the DEEMY database (http://www.deemy.de/) to gather morphological information on the exploration type (hyphal foraging distance) and rhizomorph occurrence of taxa present in our data set at > 0.5% relative abundance. Taxa exclusively forming 'abundant' rhizomorphs were scored as 'rhizomorphic', and all medium-distance exploration types were defined as 'medium distance'. Overall, we assigned morphological hyphal data for 28 ECM fungal genera, comprising more than 93% of all identified ECM fungal sequences.

Metagenomic sequence generation, processing, and annotation

Shotgun metagenomic sequencing was conducted using a NovaSeq 6000 instrument (2 × 150 bp) at the University of Michigan Advanced Genomics Core. In total, 23 203 326 006 metagenomic sequences were generated and were not merged. Filtered sequences $Q > 20$ were mapped to the UNIVEC database (bacterial, archaeal, human, viral) sequences, as well as *Q. rubra* (Konar *et al.*, 2017) and *Quercus lobata* genome assemblies (Sork *et al.*, 2016) using KRAKEN2 (v.2.0.8) with default settings (Wood *et al.*, 2019) and then removed. On average, 21.7% of sequences per sample were removed during this filtering step, yielding a mean of 307 041 274 putative fungal sequences per sample. Next, we used a direct mapping approach to annotate sequences against the CAZy and Peroxibase reference databases (100 total gene families; Table S1) using the 'sensitive' setting in DIAMOND (v.0.9.29) with an $-e$ value of 1e^{-4} (Buchfink *et al.*, 2015) and BWA-MEM (v.0.7.17) with standard settings (Li & Durbin, 2009), following recommendations for unmerged reads (Treiber *et al.*, 2020). The compiled gene database primarily contained previously defined 'core' gene families found to be actively expressed during fungal decay of SOM (Peng *et al.*, 2018; Floudas *et al.*, 2020; CAZy: http://www.cazy.org; http://peroxibase.toulouse.inra.fr/) (Table S1). We tabulated the number of near-single-copy genes, as a proxy for the number of dikaryotic genomes present in each sample, using the ORTHODB v.9 gene database, which comprised 1312 near-single-copy dikaryotic gene variants (Kriventseva *et al.*, 2019). Further methodological details are presented in Methods S1.

Statistical analysis

ECM fungal communities were rarefied to an even depth (24 021 sequences), and the responses of individual fungal genera to net N mineralization rates were examined using the TITAN2 package in R (Baker & King, 2010). We visualized variation in ECM fungal community composition using nonmetric multidimensional scaling with the R package VEGAN v.2.5-7 (Oksanen *et al.*, 2020). To isolate the effect of net N mineralization and other soil parameters in driving shifts in community composition, we used generalized dissimilarity modeling (GDM) (Ferrier *et al.*, 2007; Duhamel *et al.*, 2019). Predictors initially included in the model were net N mineralization rates, pH, soil C and N, C : N,

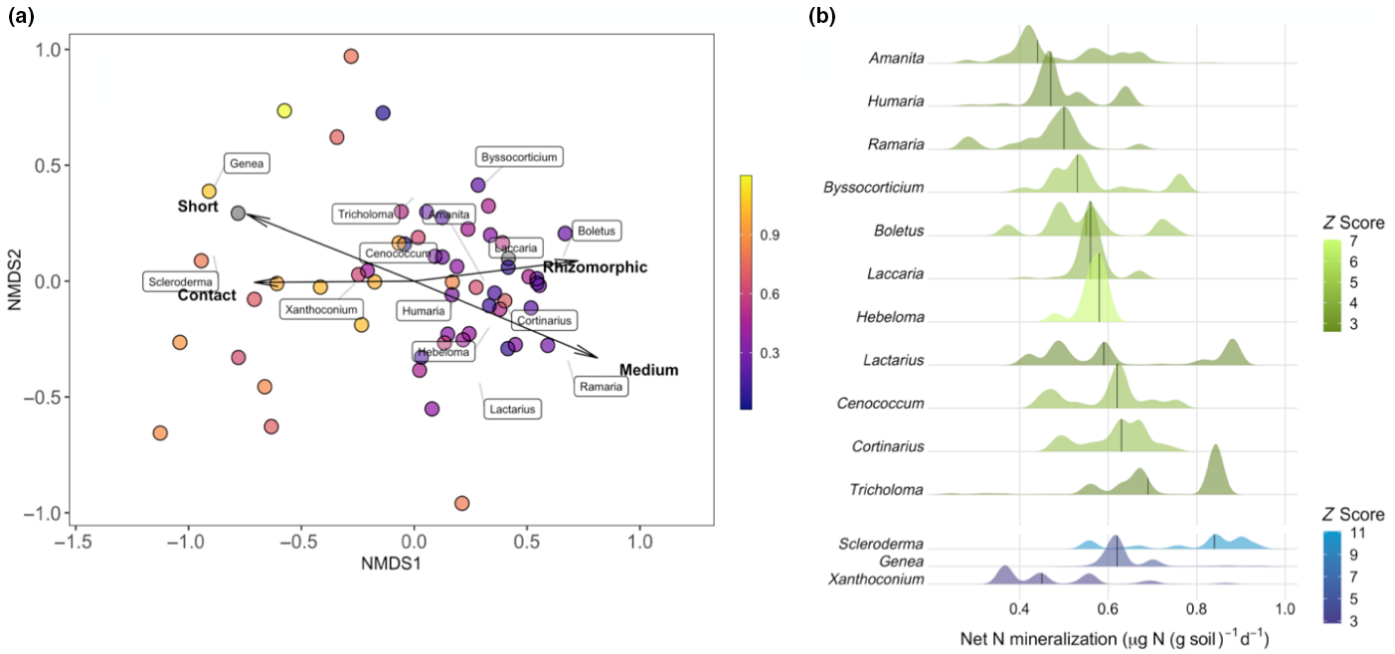

Fig. 1 (a) Nonmetric multidimensional scaling (NMDS) plot of ectomycorrhizal (ECM) fungal communities (points) inhabiting *Quercus rubra* root tips colored by rates of net N mineralization (μg N (g soil^{-1}) d^{-1}; legend bar). The vectors indicate degree of correlation between the NMDS axes and hyphal morphologies. 'Medium' and 'Short' indicate hyphal exploration types, and 'Contact' and 'Rhizomorphic' indicate presence of rhizomorphic hyphae. Plotted genus names represent scaled centroids for dominant (indicator) ECM fungal genera. (b) TITAN analysis depicting indicator ECM fungal genera. Peak along the soil gradient (*x*-axis) represents location of greatest shift in generic relative abundance. Green and blue indicate ECM fungal genera that responded negatively and positively, respectively, to rates of net N mineralization. Double peaks represent asynchronous shifts in community abundance, likely due to different underlying species responses.

TFPAs, gravimetric water availability, and Bray–Curtis transformed plant overstory dissimilarity matrix (ran separately for stem frequency or stem frequencies weighted by diameter at breast height (DBH)); this model incorporates geographic distances between individual focal trees to account for potential spatial autocorrelation. We used backwards model selection (Qin *et al.*, 2020), and we confirmed the significance of remaining predictors using matrix permutation (nperm = 500).

Gene counts derived from community-level shotgun metagenomic sequencing are weighted by the relative abundance of taxa present (Fierer *et al.*, 2012, 2014; Quinn *et al.*, 2019). To account for the inherently compositional nature of the metagenomic data, we calculated the natural logarithm of the number of sequences mapped to a given decay gene family divided by the geometric mean number of near-single-copy genes present in the sample (single-copy genes). Note that this is identical to an additive log-ratio transformation (Quinn *et al.*, 2018), which reveals how the relative abundance of decay genes present in a community behave relative to the number of single-copy genes (genomes) present in each sample. This allowed us to estimate, on average, the potential decay capacity of a hypothetical, fungal genome in each community, thereby estimating a CADT (Fierer *et al.*, 2014). Note that shotgun metagenomics allows for assessment of genotypic trait variation independent of environment impacts on expression.

We employed an extension of GDM to identify environmental and biotic predictors correlated with shifts in the compositional abundance of the 100 decay gene families. Though this is the first known employment of GDM for metagenomic community data, it is conceptually similar to modeling genomic variation across environmental gradients using single-nucleotide polymorphisms (Fitzpatrick & Keller, 2015) or nucleotide percentages for assembled genomes (Bouma-Gregson *et al.*, 2019). Standardized gene counts were Hellinger transformed (without prior log-transformation) and Euclidean distances calculated; initial environmental predictors included those described already herein, as well as a Bray–Curtis dissimilarity matrix of ECM fungal community composition. We employed a similar modeling selection procedure as already described herein. A separate GDM was run and additionally included a dissimilarity matrix (Bray–Curtis) of nonmycorrhizal fungi present, including unidentified fungal sequences totaling 512 ASVs.

We employed TITAN2 (Baker & King, 2010) to identify 'indicator' fungal gene families that responded to measures of net N mineralization using IndVal thresholds similar to previous studies of microbial 'omic responses to environmental gradients (Malik *et al.*, 2020b). We separately conducted models where soil C, and gravimetric water content were predictor variables. To account for potential non-independence among trees (samples) as a result of spatial proximity within stands, we accounted for the exact distance among trees using distances calculated from GPS coordinates. We used linear mixed effect (LME) models, taking into account the underlying spatial sampling structure, using a gaussian correlation structure as random effects. Euclidean distances

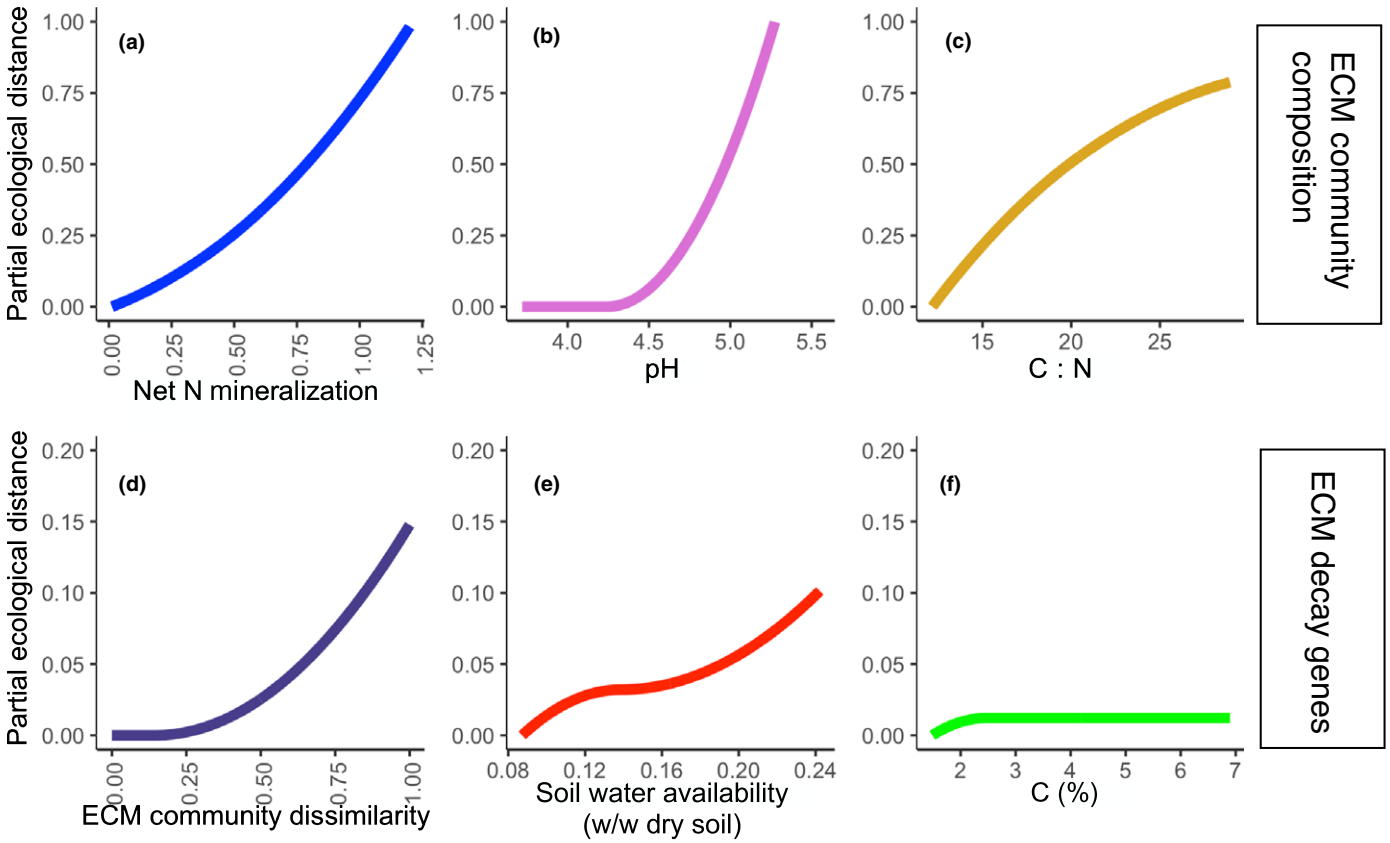

Fig. 2 Generalized dissimilarity model output depicting significant predictors of (a, b, c) shifts in ectomycorrhizal (ECM) fungal community composition and (d, e, f) metagenomic decay potential attributed to ECM fungal communities. The slope and shape of the line depict the rate of compositional change along the standardized gradient (*x*-axis). The maximum height of the regression line (on the *y*-axis) indicates the relative proportion of variance explained by each standardized variable for each analysis (row). ECM fungal communities were sampled from *Quercus rubra* root tips.

among trees were calculated and restricted maximum likelihood estimation was conducted using the package NLME 3.1 (Pinheiro *et al.*, 2017). Residuals were plotted to check for violations of normality. All statistical analyses were conducted in R v.4.0.2.

Results

The underlying soil inorganic N gradient measured using estimates of net N mineralization was temporally stable across the duration of the 2018 growing season (Fig. S2). The number of ECM fungal root-tips encountered, as well as their overall biomass, was inversely related to soil inorganic N availability (Figs S3, S4). We recovered a total of 202 ECM fungal ASVs, comprising 44 genera, of which 88% were Basidiomycetes. The proportion of sequences attributed to ECM fungal taxa was greatest under conditions of low inorganic N availability ($P = 0.053$); however, this trend is likely driven by certain outliers, because sequences that could not be identified at the genus level or had mixed trophic status (such as *Entoloma*) were not included (Tedersoo & Smith, 2013). Inclusion of *Entoloma* resulted in weaker shift in the proportion of ECM fungal sequences recovered in each sample across the gradient ($P = 0.11$). Alpha diversity measured as observed ECM fungal ASVs ranged from 9 to 50 taxa per sample and declined significantly across the soil gradient; however, Simpson's index was invariant (Fig. S5).

The morphological and compositional attributes of ECM fungal communities varied significantly across the soil inorganic N gradient (Fig. 1). For example, the relative abundance of ECM fungi possessing medium-distance exploration types ($R^2 = 0.16$, $P = 0.001$ linear fit; $t = -3.50$, $P = 0.0009$ spatial LME), and rhizomorphic hyphae were more prevalent in soils with low rates of net N mineralization ($R^2 = 0.13$, $P = 0.003$ linear fit; $t = -2.94$, $P = 0.0047$ spatial LME; Fig. 1). Importantly, the proportion of ECM fungal sequences assigned morphological attributes using DEEMY did not vary across samples ($P = 0.50$). GDM revealed that shifts in ECM fungal community composition were well explained by soil pH, rates of net N mineralization, and C : N, together explaining 36% of model deviance (Fig. 2; Table S2).

The number of metagenomic sequences that passed quality filtering steps and the sequences remaining after removal of plant and nonfungal contaminants did not significantly vary across the soil inorganic N gradient ($P = 0.36$; Fig. S6; Table S3), nor did the geometric mean number of single-copy gene sequences ($P = 0.17$; Fig. S7). The SE of single-copy sequences in each sample, a coarse metric of the evenness of genome coverage per community, also did not significantly vary ($P = 0.76$). To qualitatively compare amplicon and metagenomic-based estimates of fungal alpha

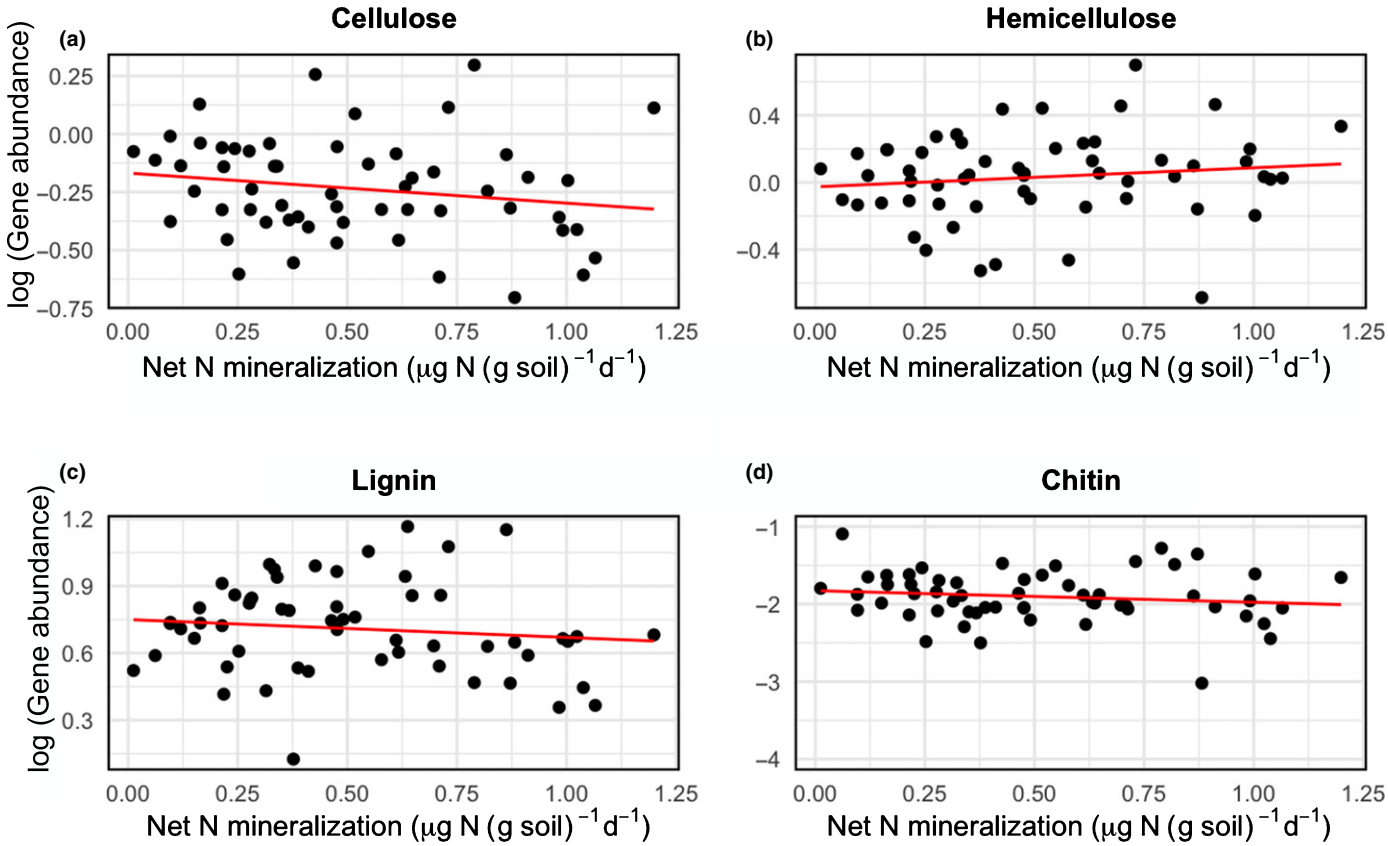

Fig. 3 Fungal gene families targeting major substrates that form soil organic matter. Points represent the summed sequence abundance of fungal genes targeting individual substrates: (a) cellulose ($t = -1.37$, $P = 0.18$); (b) hemicellulose ($t = 1.00$, $P = 0.32$); (c) lignin ($t = -1.22$, $P = 0.23$); (d) chitin ($t = -1.03$, $P = 0.31$); red trend lines represent model fit taking into account geographic sampling structure. Note distinct *y*-axis scales. Fungal genes and relationships underlying substrate responses are presented in the Supporting Information Methods S1. Fungal decay genes are primarily attributed to ectomycorrhizal fungal communities, which were sampled from *Quercus rubra* root tips.

diversity, we regressed the mean number of fungal genomes estimated using OrthoDB from metagenomic libraries against both the number of observed ECM fungal ASVs and the total number of fungal ASVs; we observed no trends for either relationship (Fig. S8). Though we cannot conclusively determine that all sequences attributed to various CAZy gene families have an ECM fungal origin, only a small proportion of non-ECM fungi (*c.* 5%) were encountered in our amplicon libraries (SE = 0.007).

We observed shifts in the relative abundance of fungal gene families active on different substrates present in SOM across the soil inorganic N gradient (Fig. 3). The presence of genes encoding enzymes active on lignin, cellulose, and chitin were greatest under conditions of low inorganic N availability (Fig. 3). For example, genes active on cellulose and chitin were 5.2 and 3.0 times more abundant respectively, under conditions of low inorganic N availability. More specifically, the relative abundance of fungal class II peroxidases and LPMOs decreased with increasing rates of net N mineralization rates (Fig. 4). MnPs were 4.9 times more abundant and genes encoding LPMOs were 2.7 times more abundant under conditions of low inorganic N availability. A total of 35 fungal gene families (Fig. S9) were identified as responsive to net N mineralization rates, including positive ($n = 20$) and negative ($n = 15$) indictor gene families (Fig. 5); many of these fungal gene families were also identified as responsive to soil C and gravimetric water content (Figs S9–S11). The summed sequence abundance of 'indicator' fungal genes that responded negatively to increasing rates of net N mineralization was significantly greater than those that responded positively to inorganic N availability (*t*-test: $t = -12.68$, $P < 0.0001$; Fig. 5).

GDM analyses revealed that soil C, gravimetric water content, and ECM fungal community dissimilarity were significant predictors of shifts in the compositional abundance of 100 gene families potentially involved in SOM decay (Fig. 2). Together, these predictors accounted for *c.* 22% of model variance; of these, ECM fungal community dissimilarity explained *c.* 63% of observed model deviance ($P = 0.066$; Table S2). When ECM fungal community composition was removed as a predictor, rates of net N mineralization remained an insignificant predictor of dissimilarity in fungal metagenomic composition. Finally, because non-ECM fungal taxa could potentially account for shifts in community gene counts (Fig. S12), we incorporated both ECM fungal and non-ECM fungal community dissimilarity matrices into a separate GDM; this model explained 27% of model deviance (Fig. S13; Table S2). Relationships between the relative abundance of individual fungal gene families and rates of net N mineralization, soil C, and gravimetric water content are

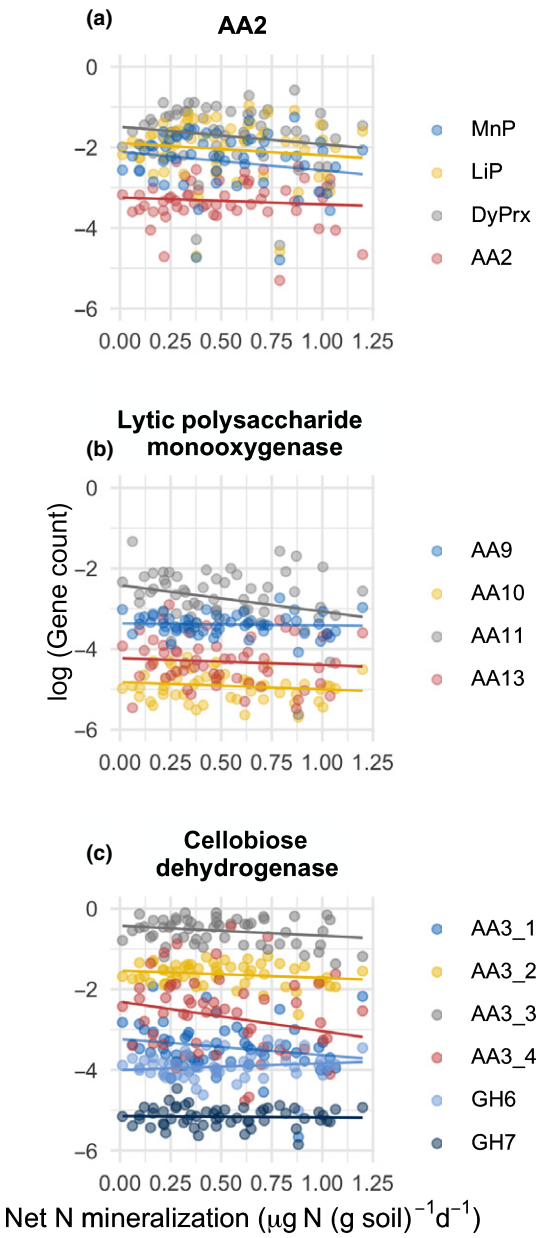

Fig. 4 Fungal gene families encoding different enzymes mediating soil organic matter decay: (a) AA2; (b) lytic polysaccharide monooxygenase; (c) cellobiose dehydrogenase. Lines represent model fit accounting for geographic spatial sampling structure. AA2 is presented for clarity, demonstrating the role of distinct gene databases. Fungal decay genes are primarily attributed to ectomycorrhizal fungal communities, which were sampled from *Quercus rubra* root tips. DyPrx, dye-decoloring peroxidase; LiP, lignin peroxidase; MnP, manganese peroxidase.

reported in Table S4. The relative sequence abundance of fungal taxa forming rhizomorphic hyphae ($t = 1.39$, $P = 0.17$) and medium-distance exploration types ($t = 1.66$, $P = 0.10$) was positively correlated with the abundance of fungal gene families that exhibited negative responses to rates of net N mineralization (negative indicator fungal gene families; $n = 15$) (Fig. 6). Negative indicator fungal gene families were 4.2 and 4.9 times more abundant where fungal taxa forming rhizomorphic hyphae and medium-distance exploration types were most common. Finally, the relative abundance of *Cortinarius* sequences was positively correlated with the summed abundance of negative 'indicator' fungal gene families (Fig. 7).

Discussion

ECM fungal assimilation of various N forms has been deemed both a response and effect trait, simultaneously impacting the outcome of assembly processes and, consequentially, ecosystem function (Koide *et al.*, 2014). In this study, we document coupled shifts in ECM fungal community composition and community-level fungal gene frequencies associated with SOM decay along a soil inorganic N gradient. These findings provide strong support for the primacy of N acquisition strategies, particularly SOM decay, in mediating ECM fungal community assembly. Overall, ECM fungal communities occurring in low inorganic N soils possessed greater genomic potential to decay SOM, and the abundance of gene families that degrade components of SOM (lignin, chitin, and cellulose) were most abundant under these conditions. Though these patterns are not causative relationships, they are congruent with models of dynamic plant adaptation to N-limited conditions via symbiosis with specialized ECM fungal communities that may obtain N-SOM. When considered alongside paired studies of *Q. rubra* responses to increasing CO_2 (Pellitier *et al.*, 2021b), our results suggest that N-SOM contributes to plant growth in a context-dependent manner, which expands existing mycorrhizal nutrient economic paradigms (Phillips *et al.*, 2013).

ECM fungal community composition was the primary determinant of fungal decay gene abundances. Moreover, because inorganic N availability was a significant driver of ECM fungal community composition it may, act as a determinant of the taxonomic and functional gene shifts observed here. Such a finding is notable because ECM fungal community turnover along both natural and polluted soil N availability gradients have been repeatedly demonstrated (Lilleskov *et al.*, 2002a; Toljander *et al.*, 2006; Cox *et al.*, 2010; van der Linde *et al.*, 2018), whereas functional shifts along soil N gradients remain poorly studied (Lilleskov *et al.*, 2002b). Overall, ECM fungal communities with the greatest decay potential were dominated by the genera *Cortinarius* and *Hebeloma*. These genera have retained some of the highest quantity of fungal genes involved in SOM decay (Bödeker *et al.*, 2009; Kohler *et al.*, 2015). We found significant correlations between the relative abundance of *Cortinarius* amplicons and the abundance of fungal genes encoding MnPs, building toward a functional perspective on the ecological niche of this widespread and diverse genus. *Cortinarius* is consistently found in low inorganic N soils (Sterkenburg *et al.*, 2015; van der Linde *et al.*, 2018), and our results are congruent with findings that this genus may actively decay SOM (Lindahl *et al.*, 2021). By contrast, so-called nitrophilic genera, commonly observed under conditions of high inorganic N availability, such as certain *Scleroderma* and *Russula* (Avis, 2012; van der Linde *et al.*, 2018), are here associated with lesser capacity to degrade SOM (Bödeker *et al.*, 2009; Kohler *et al.*, 2015; Miyauchi *et al.*, 2020). Although

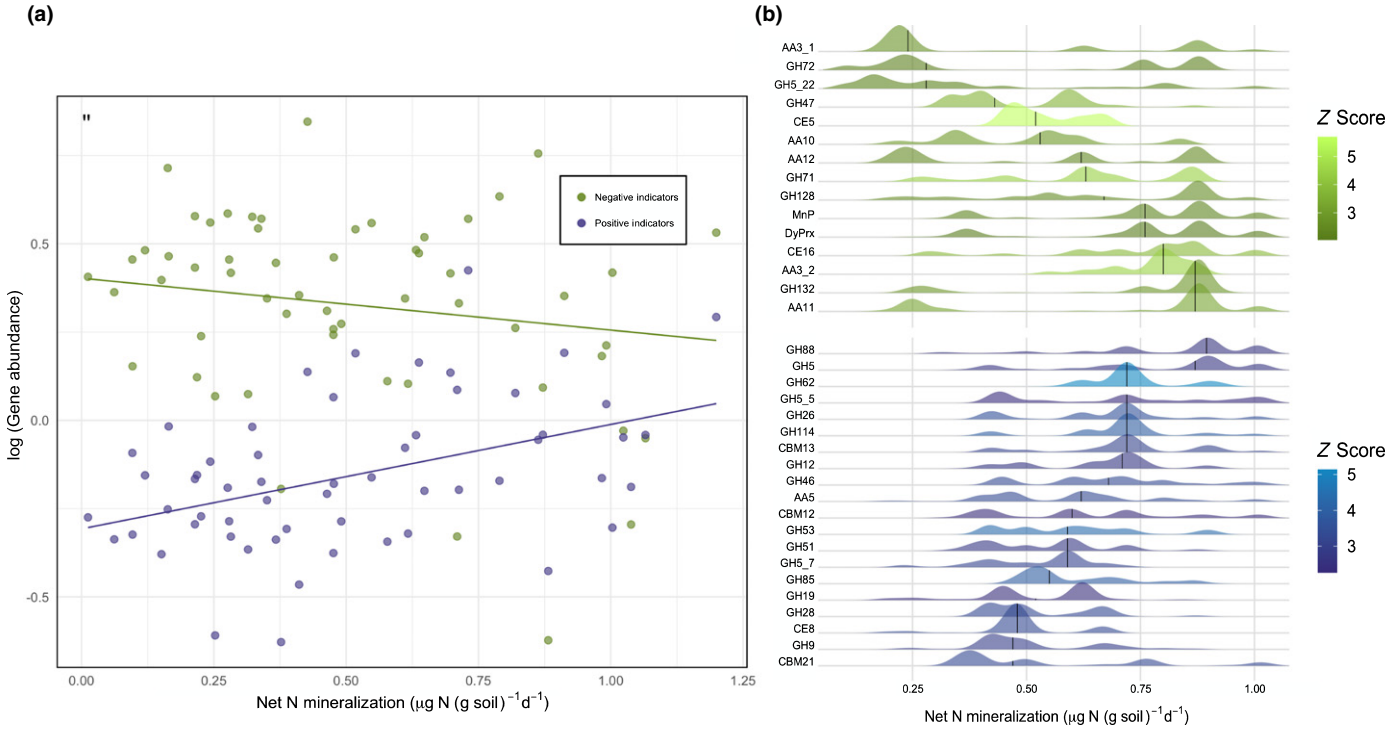

Fig. 5 (a) The relative sequence abundance of fungal decay genes predominately exhibits negative responses to increasing rates of net N mineralization. Gene families were identified and grouped as positive ($n = 20$) and negative ($n = 15$) indicators and summed. Trend lines represent statistical model fits that incorporate geographic sampling structure. (b) TITAN analysis depicts 'indicator' gene families. Peaks along the soil gradient (*x*-axis) depicts location of greatest shifts in relative gene abundance. The colors indicate the genes that responded negatively (green) or positively (blue) to rates of net N mineralization. Fungal decay genes are primarily attributed to ectomycorrhizal fungal communities, which were sampled from *Quercus rubra* root tips.

not part of this study, ECM fungal taxa associated with high inorganic N soils may be enriched in high-affinity membrane transporters that efficiently acquire NH_4 and nitrate (Javelle *et al.*, 2003; Kranabetter *et al.*, 2015).

Hyphal morpho-traits associated with N foraging exhibited parallel shifts with ECM fungal community composition and metagenomic decay potential. Taxa forming rhizomorphic and medium-distance exploration strategies dominated under conditions of low inorganic N availability. By linking metagenomic measurements of ECM fungal decay potential with turnover in hyphal morpho-traits, our study broadly supports the hypothesized role of these hyphal morphologies in the decay of SOM (Hobbie & Agerer, 2010; Moeller *et al.*, 2014; Defrenne *et al.*, 2019). Our findings are also consistent with suggestions that fungal taxa forming rhizomorphic hyphae are strong competitors under conditions in which plant access to inorganic N is scarce (Defrenne *et al.*, 2019). Such observations contribute to predictions that plants dynamically allocate C to ECM fungal symbionts that efficiently forage for N, whilst minimizing C cost (Koide *et al.*, 2014; van der Linde *et al.*, 2018).

Certain gene families with high oxidative potential occurred at greater abundance in conditions of low inorganic N availability, particularly those encoding LPMOs (AA9,10,11,13) and MnPs and dye-decoloring peroxidases. These findings provide support for the hypothesis that ECM fungal decay potential, and potentially the acquisition of N-SOM, is greatest under conditions of low inorganic N availability. LPMOs and MnPs encode primarily extracellular enzymes enabling the decay of SOM (Janusz *et al.*, 2017; Villares *et al.*, 2017) and have been the subject of recent investigations of ECM fungal SOM decay under laboratory (Doré *et al.*, 2015; Kohler *et al.*, 2015; Shah *et al.*, 2016; Nicolás *et al.*, 2019) and field conditions (Bödeker *et al.*, 2014; Sterkenburg *et al.*, 2018; Lindahl *et al.*, 2021). In addition, cellobiose dehydrogenase catalyzes the production of hydrogen peroxide (Janusz *et al.*, 2017; Sützl *et al.*, 2018) necessary for MnP activity (Hammel & Cullen, 2008) and LPMO activity (Sützl *et al.*, 2018); the abundance of these gene families (AA3_1 and AA3_2) also declined significantly with increasing soil inorganic N availability. Overall, our results highlight MnPs, one of the most potent fungal decay enzyme classes (Janusz *et al.*, 2017), as likely playing a key role in ECM fungal decay of SOM (Bödeker *et al.*, 2014; Zak *et al.*, 2019a; Lindahl *et al.*, 2021) and builds toward predictive understanding of the environmental controls governing the distribution of this decay pathway (Bödeker *et al.*, 2014; Sterkenburg *et al.*, 2018). Additionally, gene families such as CE4, CE9 and GH23, which are active on peptidoglycan, also responded negatively to increasing soil inorganic N availability. Overall, the concomitant shifts in a wide array of decay gene families along the gradient of soil inorganic N availability are notable because this supports the existence of multiple, yet potentially coupled, enzymatic decay pathways that ECM fungal communities may employ to decay the diversity of plant and microbial compounds composing SOM. Unfortunately, gene families involved in nonenzymatic Fenton decay

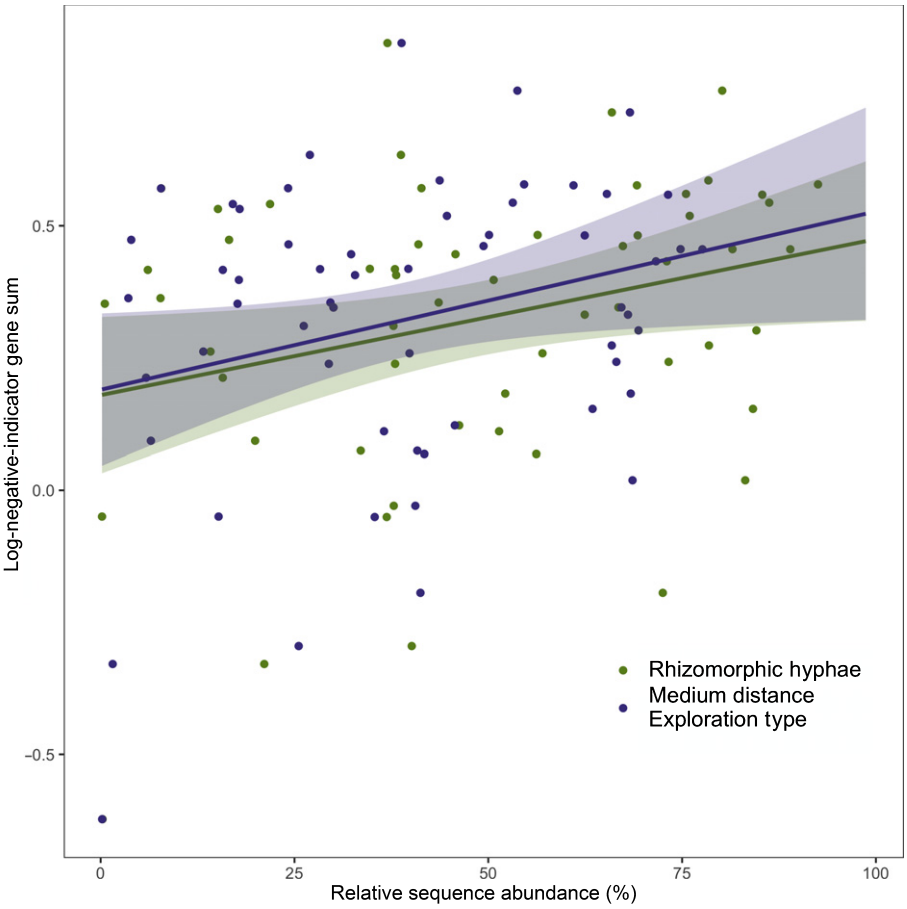

Fig. 6 Relative abundance of ectomycorrhizal (ECM) fungal hyphal foraging types (colors) and the log-transformed abundance of fungal gene families ($n = 15$) that exhibited negative responses (indicator gene families) to rates of net N mineralization: rhizomorphic ($t = 1.39$, $P = 0.17$; spatial linear mixed effect (LME)) and medium-distance exploration types ($t = 1.66$, $P = 0.10$; spatial LME). Colored bands denote SE confidence intervals. Fungal decay genes are primarily attributed to ECM fungal communities, which were sampled from *Quercus rubra* root tips.

mechanisms remain ambiguous, and further study is critical to resolve this decay process (Shah *et al.*, 2016; Janusz *et al.*, 2017; Sützl *et al.*, 2018).

Certain CAZy gene families, which are not 'functional' with respect to fitness outcomes (Shipley *et al.*, 2016), may not exhibit significant shifts across environmental gradients (Ackerly, 2003). In fact, the majority of gene families studied here exhibited minimal shifts across the inorganic N availability gradient. This does not necessarily suggest that ECM fungal communities are broadly equivalent in their capacity to decay SOM. Metagenomic investigations of microbial functional traits are generally limited by their inability to link gene frequencies with phenotypes, limiting complete understanding of trait-based environmental filtering processes shaping these communities (Ackerly, 2003). Further investigation of transcriptional regulation and enzymatic expression linked with plant uptake of N-SOM are required to fully understand plant acquisition of this critical limiting nutrient. Finally, it is critical to point out that annotation of ECM fungal genes involved in the decay of SOM is a substantial challenge because ECM fungi remain poorly represented relative to saprotrophic and pathogenic fungi in available databases.

Alongside gene families that exhibited negative and neutral responses, we observed numerous gene families that were positively correlated with increasing soil inorganic N availability. Evaluating these findings with the prevailing compositional and morphological patterns is challenging. However, certain gene families that exhibited this pattern have ambiguous activity that may not be directly involved in SOM decay. For example, certain gene families (e.g. GH5 and CE8) may play a role in mycorrhizal initiation, morphogenesis, remodeling of the fungal cell wall, or cell wall polysaccharide branching (Kües & Rühl, 2011; Blatzer *et al.*, 2020; Genre *et al.*, 2020). Gene families targeting hemicellulose also increased in relative abundance, as well as those implicated in the release of N from chitin (GH18 and GH20). We also acknowledge that certain gene families which exhibited negative responses to soil inorganic N availability, could also have alternative functions such as chitin remodeling in the fungal cell wall (AA9 or AA11).

Constraining the role of microbial communities on host tree nutrition or other biogeochemical processes (Averill *et al.*, 2014; Sulman *et al.*, 2019) requires scaling gene frequencies by estimates of microbial abundance. Similar to other studies, we documented that the number of ECM fungal root-tips decreased substantially with increasing inorganic N availability (Nilsson *et al.*, 2005; Högberg *et al.*, 2017). Qualitative scaling of genomic estimates of CADT by the abundance of ECM root-tips present in each sample further emphasizes the greater potential of ECM fungi occurring in inorganic-N-poor soils to decay SOM. Though we stress that we did not directly measure plant uptake of N-SOM, the metagenomic patterns we revealed are consistent with previous isotopic study of the same *Q. rubra* individuals. In a complementary study, we found highly ^{15}N-depleted foliage for *Q. rubra* growing under conditions of low inorganic N

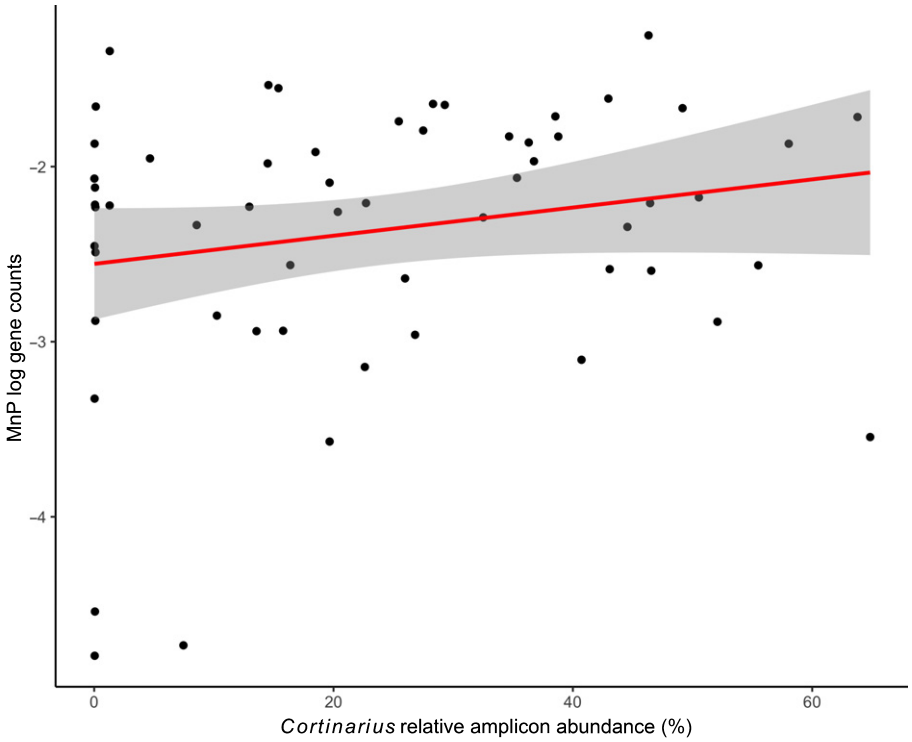

Fig. 7 The relative abundance of the ectomycorrhizal (ECM) fungus *Cortinarius* is positively correlated with the log-transformed abundance of manganese peroxidase (MnP) genes. MnP genes were normalized to the total number of putative fungal genomes present in each sample; the $P = 0.13$ linear model shown as the red line with SE shaded band. Linear mixed model accounting for potential spatial autocorrelation ($P = 0.37$). Fungal decay genes are primarily attributed to ECM fungal communities, which were sampled from *Quercus rubra* root tips.

availability and enriched foliage for *Q. rubra* occupying soils with high inorganic N availability (Pellitier *et al.*, 2021a); these patterns are broadly consistent with a transition from tree reliance on N-SOM to inorganic N uptake along the soil gradient (Kranabetter & MacKenzie, 2010).

This work represents one of the first to identify gene–trait environment linkages for microorganisms under field settings (Satinsky *et al.*, 2017; Bouma-Gregson *et al.*, 2019; Rath *et al.*, 2019; Malik *et al.*, 2020b). Consistent with expectations of trait-mediated assembly processes, metagenomic measurements of ECM fungal decay potential were tightly coupled with shifts in ECM fungal community composition along this soil inorganic N gradient. Our work provides unique support for the hypothesis that ECM fungi with enhanced SOM decay capacity are favored under conditions of low inorganic N availability (Koide *et al.*, 2014) and that ECM communities vary in their cpacity to obtain N-SOM. Our observations of shifts in the functional attributes of ECM fungal communities could represent a mechanistic basis for flexibility in plant nutrient foraging along soil N gradients, and thereby expands understanding of the organic N cycle (Kielland, 1994; Nordin *et al.*, 2004; Näsholm *et al.*, 2009). In a seminal viewpoint, Read & Perez Moreno (2003) suggested that the capacity of ECM fungi to obtain N-SOM may control the biogeography of the ECM fungal symbiosis. Our results highlight that the decay attributes of ECM fungal taxa may structure their distribution along soil inorganic N gradients.

Acknowledgements

We thank R. Upchurch, E. Herrick, K. Seguin, N. Gudal, N. Ahmad, B. VanDusen, and W. Argiroff for valuable laboratory and field support. V. Denef, M. Coon, J. Evans, and T. James provided essential sequencing and bioinformatic support. D. Goldberg and K. Peay provided comments on a draft of this manuscript. This work is supported by NSF award 1754369, and an Integrated Training in Microbial Systems (ITiMS) Fellowship to PTP. The authors declare no competing interests.

Author contributions

PTP and DRZ designed the study. PTP collected and analyzed data and wrote the manuscript with contributions from DRZ.

ORCID

Peter T. Pellitier https://orcid.org/0000-0002-0226-0784
Donald R. Zak https://orcid.org/0000-0002-9730-7337

Data availability

Raw DNA sequences associated with the ITS2 amplicon sequencing are deposited in National Center for Biotechnology Information Sequence Read Archive: SRR14164239–SRR14164298. Metagenomic sequences are deposited under accession codes SRR15377920–SRR15377978. Associated soil metadata are available in Dryad (https://doi.org/10.5061/dryad.4f4qrfjbt).

References

Ackerly DD. 2003. Community assembly, niche conservatism, and adaptive evolution in changing environments. *International Journal of Plant Sciences* **164**: S165–S184.

Ackerly DD, Cornwell WK. 2007. A trait-based approach to community assembly: partitioning of species trait values into within and among-community components. *Ecology Letters* **10**: 135–145.

Averill C, Turner BL, Finzi AC. 2014. Mycorrhiza-mediated competition between plants and decomposers drives soil carbon storage. *Nature* **505**: 543–545.

Avis PG. 2012. Ectomycorrhizal iconoclasts: the ITS rDNA diversity and nitrophilic tendencies of fetid *Russula*. *Mycologia* **104**: 998–1007.

Baker ME, King RS. 2010. A new method for detecting and interpreting biodiversity and ecological community thresholds. *Methods in Ecology and Evolution* **1**: 25–37.

Bernard-Verdier M, Navas M-L, Vellend M, Violle C, Fayolle A, Garnier E. 2012. Community assembly along a soil depth gradient: contrasting patterns of plant trait convergence and divergence in a Mediterranean rangeland. *Journal of Ecology* **100**: 1422–1433.

Blatzer M, Beauvais A, Henrissat B, Latgé J-P. 2020. Revisiting old questions and new approaches to investigate the fungal cell wall construction. In: Latgé JP, ed. *Current topics in microbiology and immunology*, vol **425**. Berlin, Heidelberg, Germany: Springer Berlin Heidelberg, 331–369.

Bödeker ITM, Clemmensen KE, de Boer W, Martin F, Olson Å, Lindahl BD. 2014. Ectomycorrhizal *Cortinarius* species participate in enzymatic oxidation of humus in northern forest ecosystems. *New Phytologist* **203**: 245–256.

Bödeker ITM, Nygren CMR, Taylor AFS, Olson Å, Lindahl BD. 2009. ClassII peroxidase-encoding genes are present in a phylogenetically wide range of ectomycorrhizal fungi. *ISME Journal* **3**: 1387–1395.

Bogar L, Peay K, Kornfeld A, Huggins J, Hortal S, Anderson I, Kennedy P. 2019. Plant-mediated partner discrimination in ectomycorrhizal mutualisms. *Mycorrhiza* **29**: 97–111.

Bouma-Gregson K, Olm MR, Probst AJ, Anantharaman K, Power ME, Banfield JF. 2019. Impacts of microbial assemblage and environmental conditions on the distribution of anatoxin-a producing cyanobacteria within a river network. *ISME Journal* **13**: 1618–1634.

Bradford MA, Wood SA, Addicott ET, Fenichel EP, Fields N, González-Rivero J, Jevon FV, Maynard DS, Oldfield EE, Polussa A *et al.* 2021. Quantifying microbial control of soil organic matter dynamics at macrosystem scales. *Biogeochemistry* **156**: 19–40.

Buchfink B, Xie C, Huson DH. 2015. Fast and sensitive protein alignment using DIAMOND. *Nature Methods* **12**: 59–60.

Callahan BJ, McMurdie PJ, Rosen MJ, Han AW, Johnson AJA, Holmes SP. 2016. DADA2: high-resolution sample inference from Illumina amplicon data. *Nature Methods* **13**: 581–583.

Christian N, Bever JD. 2018. Carbon allocation and competition maintain variation in plant root mutualisms. *Ecology and Evolution* **8**: 5792–5800.

Cornwell WK, Ackerly DD. 2009. Community assembly and shifts in plant trait distributions across an environmental gradient in coastal California. *Ecological Monographs* **79**: 109–126.

Cox F, Barsoum N, Lilleskov EA, Bidartondo MI. 2010. Nitrogen availability is a primary determinant of conifer mycorrhizas across complex environmental gradients. *Ecology Letters* **13**: 1103–1113.

Defrenne CE, Philpott TJ, Guichon SHA, Roach WJ, Pickles BJ, Simard SW. 2019. Shifts in ectomycorrhizal fungal communities and exploration types relate to the environment and fine-root traits across interior Douglas-fir forests of western Canada. *Frontiers in Plant Science* **10**: e643.

Diaz S, Cabido M, Casanoves F. 1998. Plant functional traits and environmental filters at a regional scale. *Journal of Vegetation Science* **9**: 113–122.

Doré J, Perraud M, Dieryckx C, Kohler A, Morin E, Henrissat B, Lindquist E, Zimmermann SD, Girard V, Kuo A *et al.* 2015. Comparative genomics, proteomics and transcriptomics give new insight into the exoproteome of the basidiomycete *Hebeloma cylindrosporum* and its involvement in ectomycorrhizal symbiosis. *New Phytologist* **208**: 1169–1187.

Duhamel M, Wan J, Bogar LM, Segnitz RM, Duncritts NC, Peay KG. 2019. Plant selection initiates alternative successional trajectories in the soil microbial community after disturbance. *Ecological Monographs* **89**: e01367.

Ferrier S, Manion G, Elith J, Richardson K. 2007. Using generalized dissimilarity modelling to analyse and predict patterns of beta diversity in regional biodiversity assessment. *Diversity and Distributions* **13**: 252–264.

Fierer N, Barberán A, Laughlin DC. 2014. Seeing the forest for the genes: using metagenomics to infer the aggregated traits of microbial communities. *Frontiers in Microbiology* **5**: e614.

Fierer N, Leff JW, Adams BJ, Nielsen UN, Bates ST, Lauber CL, Owens S, Gilbert JA, Wall DH, Caporaso JG. 2012. Cross-biome metagenomic analyses of soil microbial communities and their functional attributes. *Proceedings of the National Academy of Sciences, USA* **109**: 21390–21395.

Fitzpatrick CR, Copeland J, Wang PW, Guttman DS, Kotanen PM, Johnson MTJ. 2018. Assembly and ecological function of the root microbiome across angiosperm plant species. *Proceedings of the National Academy of Sciences, USA* **115**: E1157–E1165.

Fitzpatrick MC, Keller SR. 2015. Ecological genomics meets community-level modelling of biodiversity: mapping the genomic landscape of current and future environmental adaptation. *Ecology Letters* **18**: 1–16.

Floudas D, Bentzer J, Ahrén D, Johansson T, Persson P, Tunlid A. 2020. Uncovering the hidden diversity of litter-decomposition mechanisms in mushroom-forming fungi. *ISME Journal* **14**: 2046–2059.

Fry EL, Long JRD, Garrido LÁ, Alvarez N, Carrillo Y, Castañeda-Gómez L, Chomel M, Dondini M, Drake JE, Hasegawa S *et al.* 2019. Using plant, microbe, and soil fauna traits to improve the predictive power of biogeochemical models. *Methods in Ecology and Evolution* **10**: 146–157.

Genre A, Lanfranco L, Perotto S, Bonfante P. 2020. Unique and common traits in mycorrhizal symbioses. *Nature Reviews Microbiology* **18**: 1659–1660.

Hall EK, Bernhardt ES, Bier RL, Bradford MA, Boot CM, Cotner JB, del Giorgio PA, Evans SE, Graham EB, Jones SE *et al.* 2018. Understanding how microbiomes influence the systems they inhabit. *Nature Microbiology* **3**: 977–982.

Hammel KE, Cullen D. 2008. Role of fungal peroxidases in biological ligninolysis. *Current Opinion in Plant Biology* **11**: 349–355.

Hobbie EA, Agerer R. 2010. Nitrogen isotopes in ectomycorrhizal sporocarps correspond to belowground exploration types. *Plant and Soil* **327**: 71–83.

Högberg P, Näsholm T, Franklin O, Högberg MN. 2017. Tamm review: on the nature of the nitrogen limitation to plant growth in Fennoscandian boreal forests. *Forest Ecology and Management* **403**: 161–185.

Hortal S, Plett KL, Plett JM, Cresswell T, Johansen M, Pendall E, Anderson IC. 2017. Role of plant–fungal nutrient trading and host control in determining the competitive success of ectomycorrhizal fungi. *ISME Journal* **11**: 2666–2676.

Janusz G, Pawlik A, Sulej J, Świderska-Burek U, Jarosz-Wilkołazka A, Paszczyński A. 2017. Lignin degradation: microorganisms, enzymes involved, genomes analysis and evolution. *FEMS Microbiology Reviews* **41**: 941–962.

Javelle A, André B, Marini A-M, Chalot M. 2003. High-affinity ammonium transporters and nitrogen sensing in mycorrhizas. *Trends in Microbiology* **11**: 53–55.

Kielland K. 1994. Amino acid absorption by arctic plants: implications for plant nutrition and nitrogen cycling. *Ecology* **75**: 2373–2383.

Kohler A, Kuo A, Nagy LG, Morin E, Barry KW, Buscot F, Canbäck B, Choi C, Cichocki N, Clum A *et al.* 2015. Convergent losses of decay mechanisms and rapid turnover of symbiosis genes in mycorrhizal mutualists. *Nature Genetics* **47**: 410–415.

Koide RT, Fernandez C, Malcolm G. 2014. Determining place and process: functional traits of ectomycorrhizal fungi that affect both community structure and ecosystem function. *New Phytologist* **201**: 433–439.

Konar A, Choudhury O, Bullis R, Fiedler L, Kruser JM, Stephens MT, Gailing O, Schlarbaum S, Coggeshall MV, Staton ME *et al.* 2017. High-quality genetic mapping with ddRADseq in the non-model tree *Quercus rubra*. *BMC Genomics* **18**: e417.

Kranabetter JM, Hawkins BJ, Jones MD, Robbins S, Dyer T, Li T. 2015. Species turnover (β-diversity) in ectomycorrhizal fungi linked to uptake capacity. *Molecular Ecology* **24**: 5992–6005.

Kranabetter JM, MacKenzie WH. 2010. Contrasts among mycorrhizal plant guilds in foliar nitrogen concentration and δ^{15}N along productivity gradients of a boreal forest. *Ecosystems* **13**: 108–117.

Kriventseva EV, Kuznetsov D, Tegenfeldt F, Manni M, Dias R, Simão FA, Zdobnov EM. 2019. OrthoDB v10: sampling the diversity of animal, plant, fungal, protist, bacterial and viral genomes for evolutionary and functional annotations of orthologs. *Nucleic Acids Research* **47**: D807–D811.

Kües U, Rühl M. 2011. Multiple multi-copper oxidase gene families in basidiomycetes – what for? *Current Genomics* **12**: 72–94.

Lehmann J, Hansel CM, Kaiser C, Kleber M, Maher K, Manzoni S, Nunan N, Reichstein M, Schimel JP, Torn MS *et al.* 2020. Persistence of soil organic carbon caused by functional complexity. *Nature Geoscience* **13**: 529–534.

Li H, Durbin R. 2009. Fast and accurate short read alignment with Burrows–Wheeler transform. *Bioinformatics* **25**: 1754–1760.

Lilleskov EA, Fahey TJ, Horton TR, Lovett GM. 2002a. Belowground ectomycorrhizal fungal community change over a nitrogen deposition gradient in Alaska. *Ecology* **83**: 104–115.

Lilleskov EA, Hobbie EA, Fahey TJ. 2002b. Ectomycorrhizal fungal taxa differing in response to nitrogen deposition also differ in pure culture organic nitrogen use and natural abundance of nitrogen isotopes. *New Phytologist* **154**: 219–231.

Lindahl BD, Kyaschenko J, Varenius K, Clemmensen KE, Dahlberg A, Karltun E, Stendahl J. 2021. A group of ectomycorrhizal fungi restricts organic matter accumulation in boreal forest. *Ecology Letters* **24**: 1341–1351.

Lindahl BD, Tunlid A. 2015. Ectomycorrhizal fungi – potential organic matter decomposers, yet not saprotrophs. *New Phytologist* **205**: 1443–1447.

Malik AA, Martiny JBH, Brodie EL, Martiny AC, Treseder KK, Allison SD. 2020a. Defining trait-based microbial strategies with consequences for soil carbon cycling under climate change. *ISME Journal* **14**: 1–9.

Malik AA, Swenson T, Weihe C, Morrison EW, Martiny JBH, Brodie EL, Northen TR, Allison SD. 2020b. Drought and plant litter chemistry alter microbial gene expression and metabolite production. *ISME Journal* **14**: 2236–2247.

Maynard DS, Bradford MA, Covey KR, Lindner D, Glaeser J, Talbert DA, Tinker PJ, Walker DM, Crowther TW. 2019. Consistent trade-offs in fungal trait expression across broad spatial scales. *Nature Microbiology* **4**: 846–853.

McClaugherty CA, Pastor J, Aber JD, Melillo JM. 1985. Forest litter decomposition in relation to soil nitrogen dynamics and litter quality. *Ecology* **66**: 266–275.

Meeds JA, Marty Kranabetter J, Zigg I, Dunn D, Miros F, Shipley P, Jones MD. 2021. Phosphorus deficiencies invoke optimal allocation of exoenzymes by ectomycorrhizas. *ISME Journal* **15**: 1478–1489.

Miyauchi S, Kiss E, Kuo A, Drula E, Kohler A, Sánchez-García M, Morin E, Andreopoulos B, Barry KW, Bonito G *et al.* 2020. Large-scale genome sequencing of mycorrhizal fungi provides insights into the early evolution of symbiotic traits. *Nature Communications* **11**: e5125.

Moeller HV, Peay KG, Fukami T. 2014. Ectomycorrhizal fungal traits reflect environmental conditions along a coastal California edaphic gradient. *FEMS Microbiology Ecology* **87**: 797–806.

Näsholm T, Kielland K, Ganeteg U. 2009. Uptake of organic nitrogen by plants. *New Phytologist* **182**: 31–48.

Nemergut DR, Schmidt SK, Fukami T, O'Neill SP, Bilinski TM, Stanish LF, Knelman JE, Darcy JL, Lynch RC, Wickey P *et al.* 2013. Patterns and processes of microbial community assembly. *Microbiology and Molecular Biology Reviews* **77**: 342–356.

Nicolás C, Martin-Bertelsen T, Floudas D, Bentzer J, Smits M, Johansson T, Troein C, Persson P, Tunlid A. 2019. The soil organic matter decomposition mechanisms in ectomycorrhizal fungi are tuned for liberating soil organic nitrogen. *ISME Journal* **13**: 977–988.

Nilsson LO, Giesler R, Bååth E, Wallander H. 2005. Growth and biomass of mycorrhizal mycelia in coniferous forests along short natural nutrient gradients. *New Phytologist* **165**: 613–622.

Nilsson RH, Larsson K-H, Taylor AF S, Bengtsson-Palme J, Jeppesen TS, Schigel D, Kennedy P, Picard K, Glöckner FO, Tedersoo L *et al.* 2019. The UNITE database for molecular identification of fungi: handling dark taxa and parallel taxonomic classifications. *Nucleic Acids Research* **47**: D259–D264.

Nordin A, Schmidt IK, Shaver GR. 2004. Nitrogen uptake by arctic soil microbes and plants in relation to soil nitrogen supply. *Ecology* **85**: 955–962.

Oksanen J, Blanchet FG, Friendly M, Kindt R, Legendre P, McGlinn D, Minchin PR, O'Hara RB, Simpson GL, Solymos P *et al.* 2020. *vegan: community ecology package*. R package v.2.5-7. [WWW document] URL https://CRAN.R-project.org/package=vegan [accessed 12 June 2020].

Orwin KH, Kirschbaum MUF, St John MG, Dickie IA. 2011. Organic nutrient uptake by mycorrhizal fungi enhances ecosystem carbon storage: a model-based assessment. *Ecology Letters* **14**: 493–502.

Pastor J, Aber JD, McClaugherty CA, Melillo JM. 1984. Aboveground production and N and P cycling along a nitrogen mineralization gradient on Blackhawk Island, Wisconsin. *Ecology* **65**: 256–268.

Peay KG. 2016. The mutualistic niche: mycorrhizal symbiosis and community dynamics. *Annual Review of Ecology, Evolution, and Systematics* **47**: 143–164.

Peay KG, Russo SE, McGuire KL, Lim Z, Chan JP, Tan S, Davies SJ. 2015. Lack of host specificity leads to independent assortment of dipterocarps and ectomycorrhizal fungi across a soil fertility gradient. *Ecology Letters* **18**: 807–816.

Peay KG, Schubert MG, Nguyen NH, Bruns TD. 2012. Measuring ectomycorrhizal fungal dispersal: macroecological patterns driven by microscopic propagules. *Molecular Ecology* **21**: 4122–4136.

Pellitier PT, Ibáñez I, Zak DR, Argiroff WA, Acharya K. 2021a. Ectomycorrhizal access to organic nitrogen mediates CO_2 fertilization response in a dominant tree species. *Nature Communications* **12**: e5403.

Pellitier PT, Zak DR. 2018. Ectomycorrhizal fungi and the enzymatic liberation of nitrogen from soil organic matter: why evolutionary history matters. *New Phytologist* **217**: 68–73.

Pellitier PT, Zak DR, Argiroff WA, Upchurch RA. 2021b. Coupled shifts in ectomycorrhizal communities and plant uptake of organic nitrogen along a soil gradient: an isotopic perspective. *Ecosystems*. doi: 10.1007/s10021-021-00628-6.

Peng M, Aguilar-Pontes MV, Hainaut M, Henrissat B, Hildén K, Mäkelä MR, de Vries RP. 2018. Comparative analysis of basidiomycete transcriptomes reveals a core set of expressed genes encoding plant biomass degrading enzymes. *Fungal Genetics and Biology* **112**: 40–46.

Phillips RP, Brzostek E, Midgley MG. 2013. The mycorrhizal-associated nutrient economy: a new framework for predicting carbon–nutrient couplings in temperate forests. *New Phytologist* **199**: 41–51.

Pierre-Emmanuel C, François M, Marc-André S, Myriam D, Stéven C, Fabio Z, Marc B, Claude P, Adrien T, Jean G *et al.* 2016. Into the functional ecology of ectomycorrhizal communities: environmental filtering of enzymatic activities. *Journal of Ecology* **104**: 1585–1598.

Pinheiro J, Bates D, DebRoy S, Sarkar D, R Core Team. 2017. *nlme: linear and nonlinear mixed effects models*. R package v.3.1-131. [WWW document] URL https://CRAN.R-project.org/package=nlme [accessed 18 June 2020].

Qin C, Zhu K, Chiariello NR, Field CB, Peay KG. 2020. Fire history and plant community composition outweigh decadal multi-factor global change as drivers of microbial composition in an annual grassland. *Journal of Ecology* **108**: 611–625.

Quinn TP, Erb I, Gloor G, Notredame C, Richardson MF, Crowley TM. 2019. A field guide for the compositional analysis of any-omics data. *GigaScience* **8**: giz107.

Quinn TP, Erb I, Richardson MF, Crowley TM. 2018. Understanding sequencing data as compositions: an outlook and review. *Bioinformatics* **34**: 2870–2878.

Rath KM, Fierer N, Murphy DV, Rousk J. 2019. Linking bacterial community composition to soil salinity along environmental gradients. *ISME Journal* **13**: 836–846.

Ravanbakhsh M, Kowalchuk GA, Jousset A. 2019. Root-associated microorganisms reprogram plant life history along the growth–stress resistance tradeoff. *ISME Journal* **13**: 3093–3101.

Read DJ, Perez-Moreno J. 2003. Mycorrhizas and nutrient cycling in ecosystems: a journey towards relevance? *New Phytologist* **157**: 475–492.

Satinsky BM, Smith CB, Sharma S, Landa M, Medeiros PM, Coles VJ, Yager PL, Crump BC, Moran MA. 2017. Expression patterns of elemental cycling genes in the Amazon River plume. *ISME Journal* **11**: 1852–1864.

Schimel JP, Bennett J. 2004. Nitrogen mineralization: challenges of a changing paradigm. *Ecology* **85**: 591–602.

Shah F, Nicolás C, Bentzer J, Ellström M, Smits M, Rineau F, Canbäck B, Floudas D, Carleer R, Lackner G *et al.* 2016. Ectomycorrhizal fungi decompose soil organic matter using oxidative mechanisms adapted from saprotrophic ancestors. *New Phytologist* **209**: 1705–1719.

Shipley B, De Bello F, Cornelissen JHC, Laliberté E, Laughlin DC, Reich PB. 2016. Reinforcing loose foundation stones in trait-based plant ecology. *Oecologia* **180**: 923–931.

Smith SE, Read DJ. 2010. *Mycorrhizal symbiosis*. Madison WI, USA: Academic Press.

Sork VL, Fitz-Gibbon ST, Puiu D, Crepeau M, Gugger PF, Sherman R, Stevens K, Langley CH, Pellegrini M, Salzberg SL. 2016. First draft assembly and

annotation of the genome of a California endemic oak. *Genes|Genomes|Genetics* **6**: 3485–3495.

Sterkenburg E, Bahr A, Durling M, Clemmensen KE, Lindahl BD. 2015. Changes in fungal communities along a boreal forest soil fertility gradient. *New Phytologist* **207**: 1145–1158.

Sterkenburg E, Clemmensen KE, Ekblad A, Finlay RD, Lindahl BD. 2018. Contrasting effects of ectomycorrhizal fungi on early and late stage decomposition in a boreal forest. *ISME Journal* **12**: 2187–2197.

Sulman BN, Shevliakova E, Brzostek ER, Kivlin SN, Malyshev S, Menge DNL, Zhang X. 2019. Diverse mycorrhizal associations enhance terrestrial C storage in a global model. *Global Biogeochemical Cycles* **33**: 501–523.

Sützl L, Laurent CVFP, Abrera AT, Schütz G, Ludwig R, Haltrich D. 2018. Multiplicity of enzymatic functions in the CAZy AA3 family. *Applied Microbiology and Biotechnology* **102**: 2477–2492.

Taylor AFS, Martin F, Read DJ. 2000. Fungal diversity in ectomycorrhizal communities of Norway Spruce [*Picea abies* (L.) Karst.] and Beech (*Fagus sylvatica* L.) Along North-South Transects in Europe. In: Schulze E-D, ed. *Ecological studies. Carbon and nitrogen cycling in European forest ecosystems.* Berlin/Heidelberg, Germany: Springer, 343–365.

Taylor DL, Walters WA, Lennon NJ, Bochicchio J, Krohn A, Caporaso JG, Pennanen T. 2016. Accurate estimation of fungal diversity and abundance through improved lineage-specific primers optimized for Illumina amplicon sequencing. *Applied and Environmental Microbiology* **82**: 7217–7226.

Tedersoo L, Smith ME. 2013. Lineages of ectomycorrhizal fungi revisited: foraging strategies and novel lineages revealed by sequences from belowground. *Fungal Biology Reviews* **27**: 83–99.

Terrer C, Phillips RP, Hungate BA, Rosende J, Pett-Ridge J, Craig ME, van Groenigen KJ, Keenan TF, Sulman BN, Stocker BD *et al.* 2021. A trade-off between plant and soil carbon storage under elevated CO_2. *Nature* **591**: 599–603.

Terrer C, Vicca S, Hungate BA, Phillips RP, Prentice IC. 2016. Mycorrhizal association as a primary control of the CO_2 fertilization effect. *Science* **353**: 72–74.

Toljander JF, Eberhardt U, Toljander YK, Paul LR, Taylor AFS. 2006. Species composition of an ectomycorrhizal fungal community along a local nutrient gradient in a boreal forest. *New Phytologist* **170**: 873–884.

Treiber ML, Taft DH, Korf I, Mills DA, Lemay DG. 2020. Pre and post-sequencing recommendations for functional annotation of human fecal metagenomes. *BMC Bioinformatics* **21**: e74.

van der Linde S, Suz LM, Orme CDL, Cox F, Andreae H, Asi E, Atkinson B, Benham S, Carroll C, Cools N *et al.* 2018. Environment and host as large-scale controls of ectomycorrhizal fungi. *Nature* **558**: 243–248.

Villares A, Moreau C, Bennati-Granier C, Garajova S, Foucat L, Falourd X, Saake B, Berrin J-G, Cathala B. 2017. Lytic polysaccharide monooxygenases disrupt the cellulose fibers structure. *Scientific Reports* **7**: e40262.

Violle C, Navas M-L, Vile D, Kazakou E, Fortunel C, Hummel I, Garnier E. 2007. Let the concept of trait be functional! *Oikos* **116**: 882–892.

Vitousek PM, Howarth RW. 1991. Nitrogen limitation on land and in the sea: how can it occur? *Biogeochemistry* **13**: 87–115.

Wasyliw J, Karst J. 2020. Shifts in ectomycorrhizal exploration types parallel leaf and fine root area with forest age. *Journal of Ecology* **108**: 2270–2282.

Wood DE, Lu J, Langmead B. 2019. Improved metagenomic analysis with Kraken 2. *Genome Biology* **20**: 257.

Zak DR, Argiroff WA, Freedman ZB, Upchurch RA, Entwistle EM, Romanowicz KJ. 2019a. Anthropogenic N deposition, fungal gene expression, and an increasing soil carbon sink in the Northern Hemisphere. *Ecology* **100**: e02804.

Zak DR, Pellitier PT, Argiroff WA, Castillo B, James TY, Nave LE, Averill C, Beidler KV, Bhatnagar J, Blesh J *et al.* 2019b. Exploring the role of ectomycorrhizal fungi in soil carbon dynamics. *New Phytologist* **223**: 33–39.

Zak DR, Pregitzer KS. 1990. Spatial and temporal variability of nitrogen cycling in northern Lower Michigan. *Forest Science* **36**: 367–380.

Zak DR, Pregitzer KS, Host GE. 1986. Landscape variation in nitrogen mineralization and nitrification. *Canadian Journal of Forest Research* **16**: 1258–1263.

Zanne AE, Abarenkov K, Afkhami ME, Aguilar-Trigueros CA, Bates S, Bhatnagar JM, Busby PE, Christian N, Cornwell WK, Crowther TW *et al.* 2020. Fungal functional ecology: bringing a trait-based approach to plant-associated fungi. *Biological Reviews* **99**: 409–433.

Supporting Information

Additional Supporting Information may be found online in the Supporting Information section at the end of the article.

Fig. S1 Map of study sites.

Fig. S2 Mineralization rates over the course of the growing season.

Fig. S3 Colonized root-tips across the soil mineralization gradient.

Fig. S4 Freeze-dried weight of root-tips collected across the soil mineralization gradient.

Fig. S5 Alpha diversity of ectomycorrhizal communities.

Fig. S6 Metagenomic sequencing yield.

Fig. S7 Single copy gene counts per million metagenomic sequences.

Fig. S8 Abundance of fungal genomes estimated using metagenomic sequencing.

Fig. S9 Change points for negatively responding gene families to soil carbon availability.

Fig. S10 Change points for gene families responding positively to soil water availability.

Fig. S11 Change points for gene families responding negatively to soil water availability.

Fig. S12 Non-ECM fungi present in each sample.

Fig. S13 GDM with non-ECM fungi as predictor.

Methods S1 Detailed sampling and bioinformatic protocols.

Table S1 CAZy gene families, enzymes and substrates.

Table S2 Generalized dissimilarity model (GDM) output.

Table S3 Metagenomic sequence yield.

Table S4 Mixed model output of gene family responses to soil mineralization rates.

Please note: Wiley Blackwell are not responsible for the content or functionality of any Supporting Information supplied by the authors. Any queries (other than missing material) should be directed to the *New Phytologist* Central Office.